Journal of Hydrology 664 (2026) 134499

Contents lists available at ScienceDirect

Journal of Hydrology

journal homepage: www.elsevier.com/locate/jhydrol

Research papers

Grass species diversity reduces water and nutrient loss under simulated extreme precipitation

Huaqing Liu [a,b,e], Yaohui Cai [a,b,c,e,*], Xiaodong Gao [a,b,c,e], Long Ma [d], Heng Liu [c], Xining Zhao [a,b,c,e]

[a] State Key Laboratory of Soil and Water Conservation and Desertification Control, Northwest A&F University, China
[b] The Research Center of Soil and Water Conservation and Ecological Environment, Chinese Academy of Sciences and Ministry of Education, Yangling, Shaanxi 712100, China
[c] College of Soil and Water Conservation Science and Engineering, Northwest A & F University, Yangling, Shaanxi 712100, China
[d] College of Water Resources and Architectural Engineering, Northwest A & F University, Yangling, Shaanxi 712100, China
[e] University of Chinese Academy of Sciences, Beijing 100049, China

ARTICLE INFO

This manuscript was handled by Marco Borga, Editor-in-Chief, with the assistance of Kelly Kibler, Associate Editor

Keywords:
Plant diversity
Surface runoff
Carbon loss
Nitrogen loss
Extreme rainfall

ABSTRACT

Extreme precipitation events, intensified by climate change, accelerate soil erosion and threaten soil fertility. While biodiversity is known to buffer such disturbances, quantitative evidence of its role under varying rainfall intensities remains limited. Here, we conducted a simulated rainfall experiment on reconstructed grassland plots to investigate how grass species diversity (monocultures, two-, four-, and eight-species mixtures) influences runoff, infiltration, and losses of dissolved organic carbon (DOC) and dissolved inorganic nitrogen (DIN) in responses to moderate (60 mm h^{-1}) and extreme (90 and 120 mm h^{-1}) precipitation. Our results demonstrate that the eight-species mixture reduced total runoff by 39.74% and enhanced infiltration by 29.92% relative to average monoculture performance. These benefits were intensity-dependent, with runoff reductions peaking at 75.20% under moderate rainfall and infiltration enhancements reaching 54.09% during extreme events. For nutrients, the high-diversity mixture decreased DOC loss by an average of 38.09% and DIN loss by 35.06% compared to monocultures, with reductions of 65.06% (DOC) and 72.94% (DIN) at 60 mm h^{-1}, though effects diminished at higher intensities (e.g., 27.70% DOC and 24.07% DIN at 120 mm h^{-1}). Low-diversity mixtures showed inconsistent or negligible benefits, highlighting a non-linear diversity-function relationship. Structural equation modelling confirmed that species richness effects were mediated by plant community structure, particularly grass height diversity, which improved water retention and reduced nutrient leaching. These findings underscore that increasing plant diversity is a critical nature-based solution for enhancing grassland resilience and mitigating hydro-ecological degradation under intensifying precipitation extremes.

1. Introduction

Climate change and biodiversity loss represent widespread environmental and ecological crises for human societies and ecosystems (Eisenhauer, 2022; Tilman, 2000), including accelerated soil erosion which results in severe land degradation, loss of water and fertility and a decline in agricultural productivity (Borrelli et al., 2017). The increasing frequency of extreme precipitation events due to climate change is a primary driver of soil erosion (Bian et al., 2023; Chang et al., 2023; Panagos et al., 2022). Diverse plant communities can regulate water cycle processes and facilitate plant water availability, ultimately benefiting the ecosystem (Liu et al., 2025a,c). Therefore, enhancing biodiversity has the potential to increase resistance to soil and water loss under extreme rainfall events.

In water-limited areas, herbaceous vegetation has emerged as a pivotal ecological restoration strategy for soil erosion control and surface water management (Liu et al., 2020a; Wu et al., 2020). Enhanced herbaceous biodiversity further amplifies these benefits through increased biomass, nutrient retention and ecosystem resistance via resource partitioning, species facilitation, and stress buffering (Barry et al., 2019; Hector and Bagchi, 2007; Hong et al., 2022). However, the relationship between plant biodiversity and soil, water and nutrient loss

* Corresponding author at: State Key Laboratory of Soil and Water Conservation and Desertification Control, The Research Center of Soil and Water Conservation and Ecological Environment, Chinese Academy of Sciences and Ministry of Education, Yangling, Shaanxi 712100, China.

https://doi.org/10.1016/j.jhydrol.2025.134499
Received 16 February 2025; Received in revised form 7 October 2025; Accepted 27 October 2025
Available online 30 October 2025

on slope lands remains complex. While Berendse et al. (2015) reported a halving of soil loss with a fourfold increase in species richness, Allen et al. (2016) found that polycultures reduced erosion only by 23% compared to monoculture averages but failed to surpass the best-performing monoculture. This contradiction underscores broader uncertainty regarding biodiversity's efficacy, particularly given Martin et al.'s (2010) finding that functional diversity reduced sediment yield by 83% at 60% vegetation cover but increased erosion at 30% cover—highlighting minimum vegetation thresholds as essential prerequisites. Contemporary research increasingly shifts focus from taxonomic metrics to structural determinants of erosion resistance. Kervroëdan et al. (2020) identified community-weighted stem density and leaf area as dominant controls of hydraulic roughness, while Liu et al. (2022b) showed that synergistic root architectures (e.g., rhizomatic-dense plexus combinations) achieved 58.8% sediment reduction. Notably, Wen et al. (2023) confirmed this structural paradigm in China's Loess Plateau, where canopy height diversity and functional divergence explained 66% of sediment yield variance, surpassing compositional diversity effects. Collectively, these studies shift the focus of conservation science toward trait-mediated synergies and vegetation structure as primary drivers of hillslope stability.

In the field of soil erosion, controlled experiments offer a complementary approach, providing a crucial advantage for isolating the effects of plant diversity through simplified species mixtures and precise manipulation of rainfall intensity. Existing controlled experiments employing 2–3 species assemblages fail to replicate the species richness gradients (Lees et al., 2021; Liu et al., 2022a; Ma et al., 2023). Additionally, few studies have explicitly investigated the influence of plant diversity on runoff and nutrient loss under extreme rainfall. Wen et al. (2021) conducted a field experiment and demonstrated that plant diversity mitigated soil erosion as rainfall intensity increased. However, this study involved considerably lower rainfall intensities, with a 24-hour maximum of 50 mm and a 30-minute maximum of 0.7 mm min^{-1}. These are significantly less than the extreme conditions observed on the Loess Plateau (Muñoz et al., 2024), where intense rainstorms trigger substantial soil loss (Yang et al., 2021; Yue et al., 2020). Typical erosive rainfall intensity on the Loess Plateau is about 1.0 mm min^{-1} (Xu et al., 2024), with recent extreme events recording 60-minute intensities as high as 201.9 mm h^{-1}, representing an extraordinarily rare occurrence with an estimated recurrence interval of approximately 19,200 years for daily rainfall erosivity and 53,700 years for event erosivity (Xiao et al., 2023). However, intensities exceeding 120 mm h^{-1} often shift erosion processes from primarily hydraulic to gravity-driven mechanisms such as shallow landslides, particularly under high vegetation cover (Xu et al., 2024). This study focuses on hydraulic erosion processes, employing simulated rainfall intensities of 60, 90, and 120 mm h^{-1}, which are commonly used in Loess Plateau research to represent erosive and extreme events (He et al., 2024; Liu et al., 2023).

Considering these complexities, this study hypothesizes that increased plant species richness effectively mitigates surface runoff and nutrient loss under extreme precipitation conditions by enhancing biomass and canopy structure. To test this hypothesis and elucidate the underlying mechanisms, we will pursue the following objectives: 1) quantify the impact of plant diversity (1–8 species) on surface runoff under simulated extreme rainfall events (60–120 mm min^{-1}); 2) determine the influence of plant diversity on nutrient retention under extreme rainfall; 3) identify key plant characteristics that mediate the relationship between plant diversity and the control of runoff and nutrient loss.

2. Materials and methods

2.1. Experimental design

The experiment was conducted in the artificial rainfall simulation hall of the Institute of Soil and Water Conservation, Chinese Academy of Sciences. We utilized side-spray artificial rainfall simulator located in Zone 2 of the facility. This system is designed to replicate the erosive characteristics of natural rainfall in the region (Zhou et al., 2000). It consists of two opposing banks of nozzles, each containing four distinct orifice plates (diameters: 7, 11, 13, and 15 mm) to precisely modulate intensity. The nozzles are installed at a height of 14.5 m and spray water upwards, achieving a total fall height of approximately 16 m. This ensures that raindrops, with a maximum diameter of 5 mm, reach over 95% of their terminal velocity, thus closely mimicking the kinetic energy of natural erosive storms (Laws, 1941; Zhou et al., 2000). The opposing-spray design ensures high rainfall uniformity across the total rainfall area of 6 m × 3 m = 18 m^2. The experimental soil tank dimensions were 1.5 m × 1.2 m × 0.8 m (length × width × height, Fig. 1). The soil tank was divided longitudinally in the middle, with a collection trough at the lower end for collecting surface runoff and sediment. The soil used was silt loam (28.54% sand, 59.68% silt, and 11.78% clay particles), obtained from abandoned land in Ansai County, Yan'an City, Shaanxi Province. The soil was air-dried to a moisture content of approximately 10%, passed through a 10 mm sieve, and all visible plant roots, stones, or other debris were removed. During soil filling, a layer of gauze was first placed at the bottom of the tank, followed by a 5 cm layer of fine sand, and then two more layers of gauze to ensure uniform water infiltration (Liu et al., 2020b). In May 2021, the soil was packed to a total depth of 60 cm in six layers of 10 cm each, with a bulk density of approximately 1.3 g cm^{-3}, compacting each layer during filling. After each layer was packed, a scraper was used to smooth the surface before filling the next layer. During this process, two 100 cm long Trime tubes were installed at 50 cm and 100 cm from the top of the soil tank for soil moisture measurements during the early stages of the experiment. To ensure consistent initial soil moisture conditions before sowing, each soil tank was saturated with water (until water overflowed from the bottom of the tank) after filling. The tanks were then left to settle naturally outdoors for three months to simulate natural conditions.

We selected eight grass species for sowing based on three criteria: 1) prioritizing native species with strong adaptability and excellent soil and water conservation functions; 2) trait complementarity based on morphology, phenology, and physiological characteristics to maximize functional diversity; and 3) easy accessibility and availability of seeds for large-scale promotion and planting. These selection criteria were informed by biodiversity-ecosystem functioning research demonstrating that species mixtures with contrasting functional traits enhance hydrological performance (Liu et al., 2025b; Weisser et al., 2017). Based on these criteria, eight grass species were selected for this study: Alfalfa (*Medicago sativa*, MS), *Astragalus adsurgens* (AA), Sweet clover (*Melilotus officinalis (L.) Pall.*, MP), *Lespedeza daurica* (LD), Smooth bromegrass (*Bromus inermis Leyss.*, BL), *Elymus dahuricus Turcz.* (ET), Crested wheatgrass (*Agropyron cristatum (L.) Gaertn.*, AG), and *Viola philippica* (VP). Functionally, these species represent key groups: legumes (MS, AA, MP, and LD), grasses (BL, ET, and AG), and forbs (VP).

The 11 treatment combinations were strategically designed following established biodiversity research protocols to test specific hypotheses about diversity-functioning relationships: single species of MS (S11), AA (S12), BL (S13), and ET (S14), two species mixtures of AA + BL (M21), MS + ET (M22), MP + BL (M23), LD + ET (M24), four species mixtures of AA + MS + BL + ET (M41) and LD + MP + BL + ET (M42), eight species mixture (M8), and no plant as control (CK). These combinations encompassed four plant diversity gradients: 1, 2, 4, and 8. The specific species and their pairings were informed by our research group's previous studies investigating these plant communities and their hydrological impacts (Liu et al., 2024, 2025b). For instance, two-species mixtures were deliberately designed to pair a nitrogen-fixing legume with a fibrous-rooted grass (e.g., AA + BL), a well-established strategy to enhance both soil fertility and structure, thereby testing for synergistic effects on hydrological regulation. The sowing method was uniform broadcasting, with a seeding density of 1000 viable seeds m^{-2}. The emergence rate was determined experimentally in the early stages. In

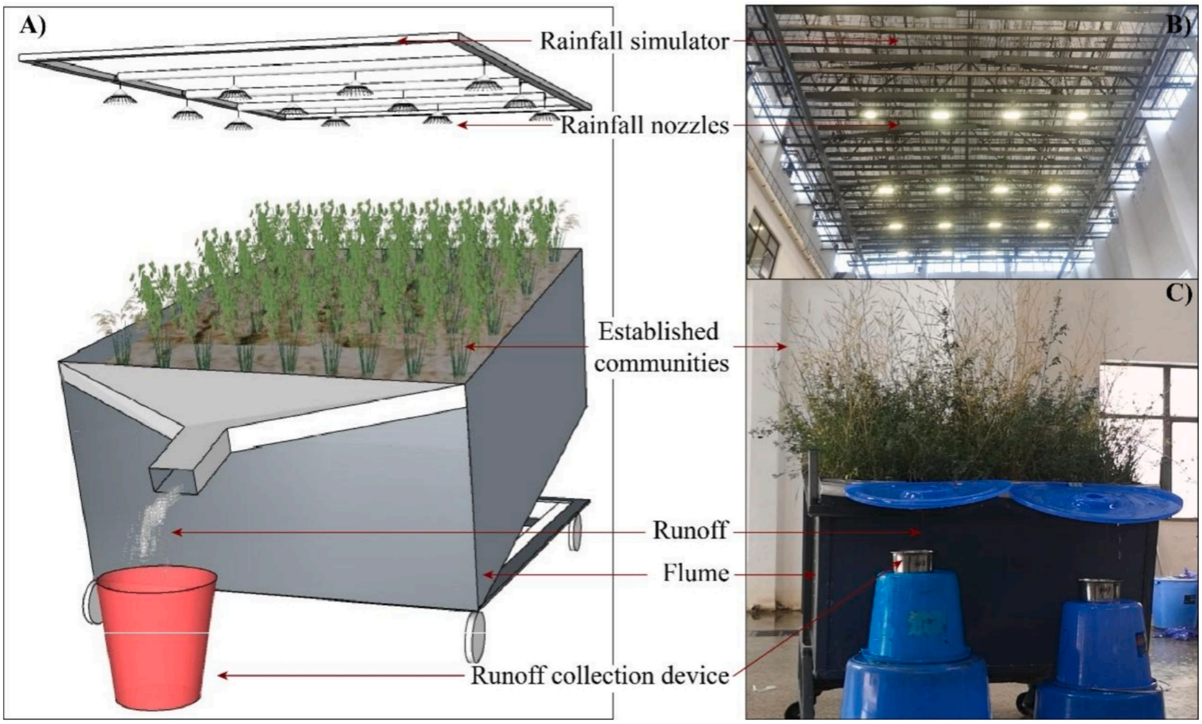

Fig. 1. Rainfall simulation experimental setup showing the side-spray artificial rainfall system. (A) Diagram of the controlled rainfall simulation system, (B) Real rainfall simulator and nozzles, (C) Diverse plant communities under simulated extreme precipitation.

the mixed treatments, the proportion of each species was equal. For example, in the mixture of MS and ET, the number of viable seeds of each species accounted for half of the total, and other treatments were similar.

The experiment was structured as a randomized block design with repeated measures on each soil tank. The eight-species mixture and bare soil control were established in four replicate soil tanks (n = 4). All other treatments—including the four monocultures, four two-species mixtures, and two four-species mixtures—were established in two replicate tanks each (n = 2). This resulted in a total of 28 independent experimental plots. Each of these 28 plots was sequentially subjected to all three rainfall intensities (60, 90, and 120 mm h^{-1}), representing the repeated measures. The order of intensity application was randomized for each plot to control for potential temporal bias. A minimum 72-hour recovery period separated consecutive rainfall events on the same plot to ensure soil hydrological reset. This design yielded a total of 84 experimental runs.

The experiment was conducted on a 12° slope, which represents a moderate gradient within the range of slopes characteristic of erosion-prone areas in the Loess Plateau region (Zheng, 2006). This slope angle is commonly used in soil erosion studies and is representative of hillslopes where grassland restoration is typically implemented (Shang et al., 2020; Shi et al., 2015). Considering the characteristics of heavy rainfall events in the Loess Plateau and the frequent occurrence of extreme rainfall in recent year (Dong et al., 2015), three rainfall intensities were chosen for the simulated rainfall: 60, 90, and 120 mm h^{-1}, with a duration of 60 min. Soil moisture was measured using a Trime-IPH tube-type TDR soil moisture measurement system before the rainfall event.

2.2. Rainfall simulations and measurements

Rainfall protocols followed standardized procedures. Pre-rainfall of 30 mm h^{-1} was applied 24 h prior to the experiments to achieve a 15% gravimetric soil water content. Target rainfall intensity was calibrated using six rain gauges positioned across the plot area. After surface runoff initiation, all runoff samples were collected continuously in 500 ml plastic buckets, which were exchanged every 4 min. Runoff volume was determined gravimetrically (±0.1 g precision), and sediment yield was quantified via oven-drying at 55℃ for 72 h. Runoff samples were immediately filtered through 0.45 μm membranes and stored at 4℃. Within one week, TOC of the runoff samples was determined using a Shimadzu TOC-L CPH total organic carbon analyzer (Shimadzu Corp., Kyoto, Japan), and nitrate and ammonium nitrogen concentrations were measured using a Skalar San++ continuous flow analyzer (Skalar Analytical B.V., Breda, The Netherlands). Due to minimal sediment generation during most rainfall events, insufficient sediment particles were collected for reliable weight and nutrient content analysis. Therefore, sediment-bound carbon and nitrogen losses were not quantified in this study.

2.3. Plant biomass and trait measurements

After the simulated rainfall experiments, the plots were left for five days to allow surface water to evaporate. Subsequently, biomass and plant traits were measured. Within each plot, three 25 cm × 25 cm quadrats were randomly placed to sample plant traits. Within each quadrat, all individuals were identified to the species level. For each species present, we measured up to six randomly selected individuals (or all individuals if fewer than six were present). Plant height was measured as the maximum natural vertical distance from the soil surface to the highest photosynthetic tissue using a ruler (1 mm accuracy). Basal diameter was measured at 2 cm above the soil surface using an electronic vernier caliper (0.01 mm accuracy). Following trait measurements, fresh aboveground plant biomass was measured by clipping the plants at a height of 5 cm.

2.4. Data analysis

2.4.1. Runoff, infiltration and nutrient loss rates

Runoff rate was calculated using the following formula (Yang et al., 2021):

$$R = \frac{V}{T \times A \times \cos\theta} \tag{1}$$

where, R is the runoff rate, mm min^{-1}; V is the runoff volume at the outlet for the given time interval, L; A is the plot area, m^2; T is the sampling time, min; θ is the slope gradient, degrees.

Infiltration rate was calculated using the following formula (Yang et al., 2021):

$$IR = RI - \frac{V}{T \times A \times \cos\theta} - Interception \tag{2}$$

where, RI is the infiltration rate, mm min^{-1}; RI is the rainfall intensities, mm min^{-1}.

The dissolved organic carbon loss rate (TOCR, mg·m^{-2}·min^{-1}), NH_4-N loss rate (NH_4-NR, mg·m^{-2}·min^{-1}) and NO_3-N loss rate (NO_3-NR, mg·m^{-2}·min^{-1}) were calculated as:

$$TOC_R = \frac{DOCC \times Q}{T \times A \times \cos\theta} \tag{3}$$

$$NH_4 - N_R = \frac{NH_4 - N_C \times Q}{T \times A \times \cos\theta} \tag{4}$$

$$NO_3 - N_R = \frac{NO_3 - N_C \times Q}{T \times A \times \cos\theta} \tag{5}$$

2.4.2. Runoff and nutrient reduction effectiveness

The runoff reduction efficiency (R_{GR}) relative to bare soil was calculated as:

$$R_{GR} = \frac{R_B - R_{Gi}}{R_B} \tag{6}$$

where R_B is the runoff from the bareland slope; R_{Gi} is the runoff from the grass treatment of i th species number.

The species richness runoff reduction (R_{SRR}) relative to the average of the monocultures was calculated as:

$$R_{SRR} = \frac{R_S - R_{Mj}}{R_S} \tag{7}$$

where R_S is the runoff from the single species slope; R_{Mi} is the runoff from the mixture species of j th species number.

2.4.3. Structural diversity

Grass height diversity (GHD) and basal diameter diversity (BDD)—key structural components influencing surface roughness and overland flow dynamics—were quantified to characterize the plant community's structural diversity in relation to runoff generation. While GHD primarily affects canopy interception, BDD, reflecting surface roughness, reduces flow velocity and increases infiltration by creating microtopographic barriers. GHD was assessed using 10 cm height classes ranging from 10 to 130 cm (10–20, 20–30…120–130 cm). BDD was assessed using classes ranging from <0.5 cm to 6 cm (in 0.5 cm increments). The Shannon diversity index was used for both calculations:

$$GHD = -\sum_{i=1}^{h} p_i \times \ln(p_i) \tag{8}$$

$$BDD = -\sum_{j=1}^{d} p_j \times \ln(p_j) \tag{9}$$

where, p_i and p_j are the proportions of ith height classes and jth basal diameter classes, while h and d are the number of the height classes and basal diameter classes.

2.4.4. Statistical analysis

A two-way analysis of variance with Duncan's multiple comparisons test was used to test the effects of species richness and rainfall intensity on runoff, infiltration, TOC loss and DIN loss using the R package *agricolae* (Mendiburu, 2023). Simple linear regressions were conducted between plant traits and hydrological responses using the R package *ggpubr* (Kassambara, 2023). To elucidate the causal pathways by which plant traits influenced runoff, infiltration, and nutrient loss, we fitted piecewise structural equation model (SEM) using the R package *piecewiseSEM* (Lefcheck, 2016). Species richness was log-transformed to meet assumptions of normality and homoscedasticity (Hurtado et al., 2024). All analyses were carried out in R version 4.3.1 (R Core Team, 2023).

3. Results

3.1. Runoff and infiltration

Figs. 2 and 3 show the runoff and infiltration dynamics, respectively, under different diversity treatments and rainfall intensities. Across all intensities, the eight-species mixture consistently exhibited the lowest runoff and highest infiltration, while bare soil plots showed the opposite trend (earliest runoff initiation, largest runoff volume, earliest decline in infiltration rate, and lowest infiltration volume).

At 60 mm h^{-1}, the eight-species mixture delayed runoff initiation and minimized runoff volume compared to other treatments. Single-species treatments showed variable runoff responses, with *Bromus inermis Leyss.* (BL) exhibiting the highest runoff volume among them. At higher rainfall intensities (90 mm h^{-1} and 120 mm h^{-1}), all vegetated treatments exhibited a runoff process that initially increased and then stabilized, whereas bare soil plots showed a different pattern. Across all treatments, higher rainfall intensity led to higher runoff rates.

At 60 mm h^{-1} rainfall intensity, the eight-species mixture and the four-species mixture (LD + MP + BL + ET) initially infiltrated all precipitation, delaying the onset of infiltration rate decline. In contrast, bare soil showed the earliest decline in infiltration. At 90 mm h^{-1} and 120 mm h^{-1}, all vegetated plots, excluding the bare soil control, exhibited an initial period of complete infiltration before rates declined and stabilized.

Fig. 4 quantifies the differences in total runoff and infiltration. Bare soil consistently had the highest total runoff volume and lowest total infiltration volume across all three rainfall intensities. The eight-species mixture significantly reduced runoff and increased infiltration compared to bare soil and single-species treatments. For example, compared to bare soil, the eight-species mixture reduced runoff by 93.76%, 50.23%, and 53.59% at 60 mm h^{-1}, 90 mm h^{-1}, and 120 mm h^{-1}, respectively. Two-species mixture generally performed worse than single-species treatments in terms of runoff reduction and infiltration enhancement, while the four-species mixture showed mixed results depending on rainfall intensity. Compared to single-species treatments, the eight-species mixture reduced runoff by 75.20%, 19.11%, and 24.91% at 60 mm h^{-1}, 90 mm h^{-1}, and 120 mm h^{-1}, respectively. Concurrently, this mixture consistently enhanced infiltration, with increases of 5.79%, 29.88%, and 54.09% at respective rainfall intensities.

3.2. Dissolved organic carbon and inorganic nitrogen loss via runoff

The DOC loss rates under different diversity treatments and rainfall intensities, as shown in Fig. 5, varied with runoff generation during rainfall events. At a rainfall intensity of 60 mm h^{-1}, significant differences in DOC loss were observed between species combinations and diversity treatments. The combination of LD + MP + BL + ET (four species mix) exhibited the lowest DOC loss rate, followed by the eight-species mixture. In contrast, the AA + MS + BL + ET combination showed higher DOC loss, with a distinctive pattern of initially high loss followed by a decrease. On bare soil slopes, DOC loss increased in the early stages and then leveled off, while DOC concentration remained stable and lower than that of vegetated slopes throughout the runoff process. Among single species treatments, there were notable

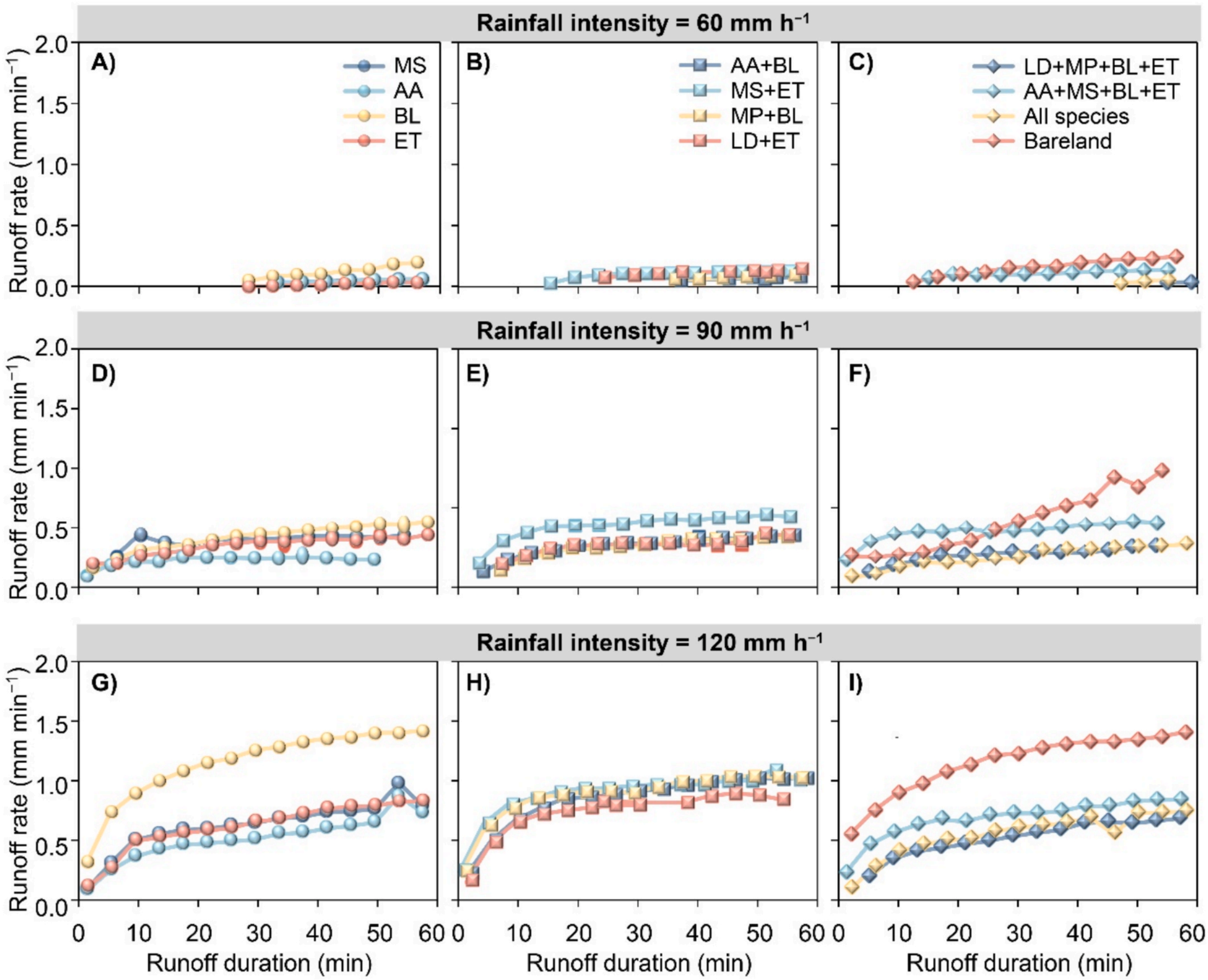

Fig. 2. Runoff rate processes under different species combined treatments and rainfall intensities. Runoff rate was measured for monocultures (A, D, G), two-species mixtures (B, E, H), and multi-species mixtures including all species and bare land (C, F, I) during simulated rainfall events at intensities of 60 mm h^{-1} (A–C), 90 mm h^{-1} (D–F), and 120 mm h^{-1} (G–I). MS, *Medicago sativa*; AA, *Astragalus adsurgens*; BL, *Bromus inermis*; ET, *Elymus dahuricus*; MP, *Melilotus officinalis*; LD, *Lespedeza daurica*.

differences: the DOC loss rate for BL showed an overall increasing trend with fluctuations, while ET demonstrated a gradual increase, and MS and AA maintained relatively stable DOC loss rates. At a rainfall intensity of 90 mm h^{-1}, DOC loss rates for MS, AA, and the AA + MS + BL + ET mixture were highest at the beginning and gradually decreased before stabilizing, while other treatments remained relatively steady. At 120 mm h^{-1}, the DOC loss rates for the four single-species treatments and the AA + BL mixture fluctuated significantly. In all treatments, higher rainfall intensities led to greater DOC losses.

The DIN (Dissolved inorganic nitrogen) loss rates under varying diversity treatments and rainfall intensities, illustrated in Fig. 6, show distinct patterns of runoff-generated loss. At a rainfall intensity of 60 mm h^{-1}, significant differences appeared among species combinations and diversity treatments in terms of DIN loss. The LD + MP + BL + ET four-species mixture had the lowest DIN loss rate, followed by the eight-species mixture. In contrast, the AA + MS + BL + ET combination exhibited higher DIN loss, starting stable and then increasing, distinguishing it from other treatments. On bare soil slopes, the DIN loss rate gradually increased throughout the rainfall event. For single species treatments, the DIN loss rates varied greatly: BL treatment showed an overall increasing trend, ET treatment had a gradual rise, while MS and AA treatments remained stable. At a rainfall intensity of 90 mm h^{-1}, the DIN loss rates for MS and MS + ET were initially the highest, then decreased and stabilized, whereas other treatments were relatively stable. When the intensity reached 120 mm h^{-1}, the DIN loss rates for single species and the AA + BL mixture fluctuated significantly.

The bare soil slopes exhibited higher DOC losses at 60 mm h^{-1} and 120 mm h^{-1} compared to vegetated slopes, but lower DOC losses at 90 mm h^{-1}. The total DOC loss from bare soil slopes was 17.12, 21.67, and 180.45 mg m^{-2} min^{-1} at rainfall intensities of 60 mm h^{-1}, 90 mm h^{-1}, and 120 mm h^{-1}, respectively. Among all vegetated treatments, the eight-species mixture had the lowest total DOC loss, showing the greatest reduction in DOC loss compared to bare soil slopes, with reductions of 90.30%, 21.74%, and 67.58% at 60 mm h^{-1}, 90 mm h^{-1}, and 120 mm h^{-1}, respectively (Fig. 7). Compared to monocultures, two-species mixtures increased DOC loss under all three rainfall intensities, while four-species mixtures increased DOC loss at 60 mm h^{-1} and 90 mm h^{-1} but reduced it at 120 mm h^{-1}. The eight-species mixture consistently reduced DOC loss, with reductions of 65.06%, 21.50%, and 27.70% compared to single-species treatments at 60 mm h^{-1}, 90 mm

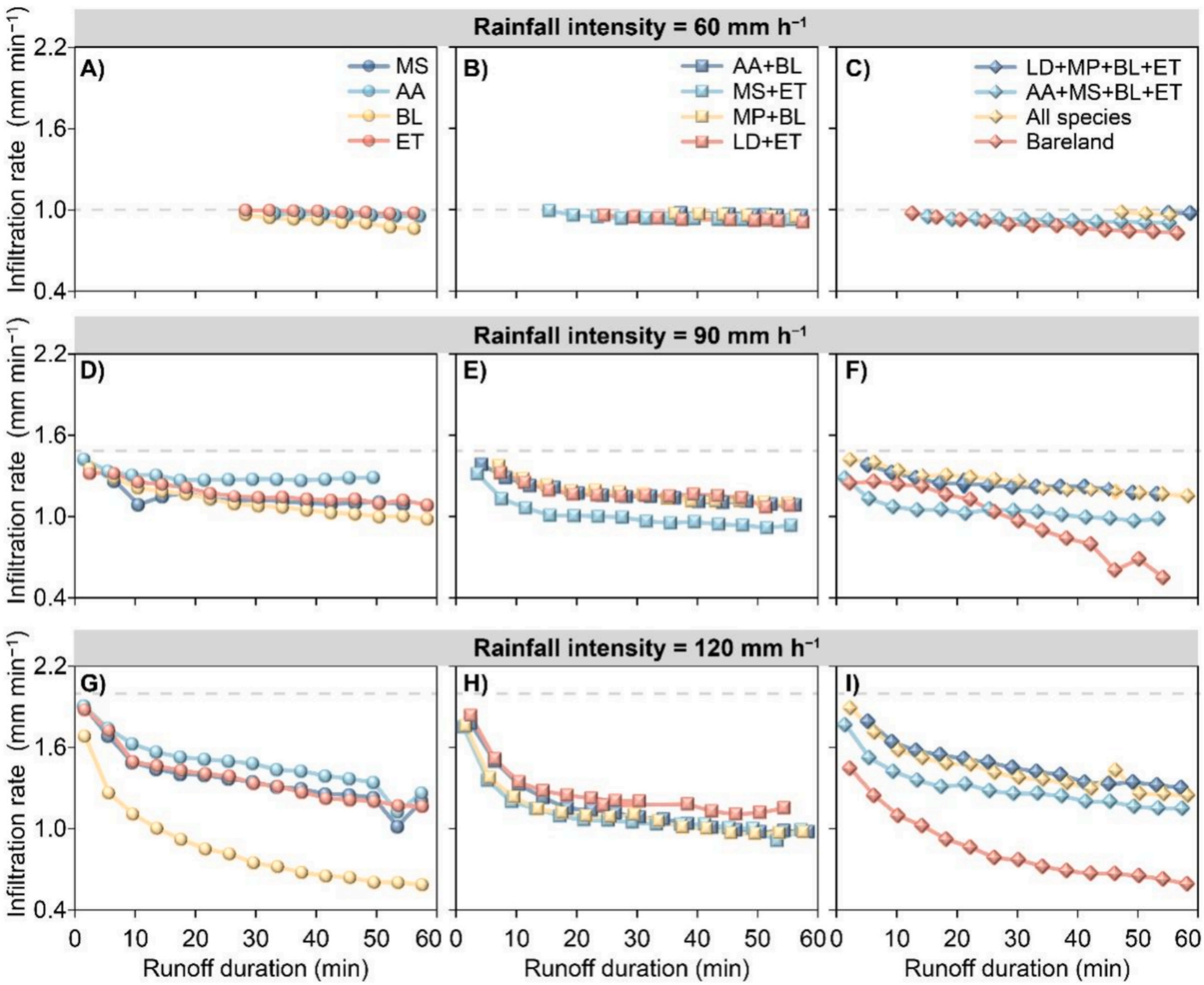

Fig. 3. Infiltration rate processes under different species combined treatments and rainfall intensities. Infiltration rate was measured for monocultures (A, D, G), two-species mixtures (B, E, H), and multi-species mixtures including all species and bare land (C, F, I) during simulated rainfall events at intensities of 60 mm h^{-1} (A–C), 90 mm h^{-1} (D–F), and 120 mm h^{-1} (G–I). MS, *Medicago sativa*; AA, *Astragalus adsurgens*; BL, *Bromus inermis*; ET, *Elymus dahuricus*; MP, *Melilotus officinalis*; LD, *Lespedeza daurica*.

h^{-1}, and 120 mm h^{-1}, respectively.

Across all treatments, the maximum DIN loss occurred at 90 mm h^{-1}, followed by 120 mm h^{-1}, with 60 mm h^{-1} being the lowest. On bare soil slopes, the DIN loss was higher at 60 mm h^{-1} and 90 mm h^{-1} than on vegetated slopes, but lower at 120 mm h^{-1}. The total DIN loss for bare soil was 33.65, 277.75, and 71.58 mg m^{-2} under rainfall intensities of 60 mm h^{-1}, 90 mm h^{-1}, and 120 mm h^{-1}, respectively. Among all vegetated treatments, the eight-species mixture had the lowest total DIN loss and the largest reduction compared to bare soil: 95.73%, 34.94%, and –23.67% at 60 mm h^{-1}, 90 mm h^{-1}, and 120 mm h^{-1}, respectively. Compared to monocultures, two-species mixtures increased DIN loss across all rainfall intensities, while four-species mixtures increased DIN loss at 60 mm h^{-1} and 90 mm h^{-1} but reduced it at 120 mm h^{-1}. The eight-species mixture consistently reduced DIN loss, with reductions of 72.94%, 8.17%, and 24.07% compared to single-species treatments at 60 mm h^{-1}, 90 mm h^{-1}, and 120 mm h^{-1}, respectively.

3.3. Relationship between plant traits and runoff, TOC and nitrogen loss

The results of the simple linear regression analysis indicate that under a rainfall intensity of 60 mm h^{-1}, biomass serves as a significant predictor for runoff volume and total organic carbon (TOC) loss (Fig. 8). At a rainfall intensity of 90 mm h^{-1}, biomass proves to be an important predictor for runoff volume, infiltration, and dissolved inorganic nitrogen (DIN) loss. Moreover, grass height diversity (GHD) is identified as a crucial predictor for runoff volume, infiltration, TOC loss, and DIN loss at a rainfall intensity of 60 mm h^{-1}, whereas under a rainfall intensity of 120 mm h^{-1}, GHD alone can directly predict runoff volume and infiltration. DOC decreased with biomass at 60 mm h^{-1} and 90 mm h^{-1} but increased at 120 mm h^{-1}. Similar, the relationship between DOC and BDD shown the same pattern. These results were consistent with our SEMs (Fig. 9). Our SEMs reveal that the impact of plant diversity on surface runoff, infiltration, and nutrient loss processes is primarily mediated through effects associated with GHD. Under rainfall intensities of 60 mm h^{-1} and 90 mm h^{-1}, biomass directly affects runoff volume, while at 120 mm h^{-1}, biomass does not influence runoff volume; instead, basal diameter diversity (BDD) exerts a direct influence.

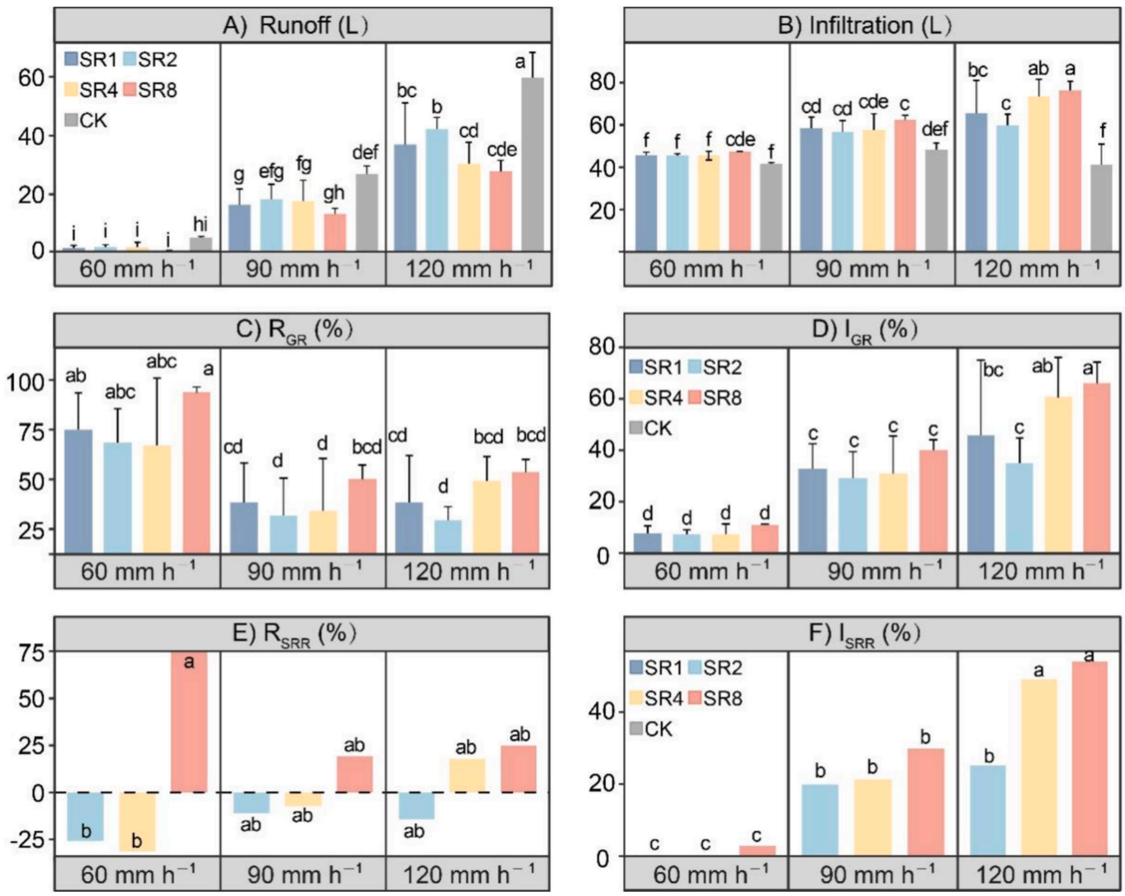

Fig. 4. The percentage decrease of runoff (A, D, E) and increase of total infiltration (B, D, F) under different species richness and rainfall intensities. Different lowercase letters near error bars indicate a significant difference among rainfall intensities and species number at the $p < 0.05$ level.

4. Discussion

4.1. *Grass species diversity controls runoff and infiltration via structural mechanisms*

This study reveals that grass species diversity regulates runoff and infiltration under extreme rainfall, with canopy structural diversity—not biomass—emerging as the dominant mediator. Contrary to studies emphasizing biomass effects (Allen et al., 2016; Berendse et al., 2015), our findings show that grass height diversity (GHD) emerged as the primary mediator. While diverse treatments increased biomass, no mixture out-yielded the top-performing monocultures, reflecting strong selection effects common in biodiversity experiments driven by (Cardinale et al., 2007).

Mechanistically, higher GHD communities create multi-layered canopies that intercept rainfall iteratively, reducing raindrop kinetic energy (Jiang et al., 2024; Zhang et al., 2020), whereas single-layer canopies (particularly tall monocultures) prove less effective as raindrops reach terminal velocity (Geißler et al., 2012). This structural advantage intensifies under extreme rainfall (90 and 120 mm h^{-1}), a condition that increases canopy penetration (Nanko et al., 2008). This intensification explains why diversity effects were amplified at higher intensities in our study—a finding consistent with previous research (Zhao et al., 2014a,b).

Beyond canopy structure, diverse plant communities influence hydrological processes through complementary structural traits, including those related to stems, litter and roots (Li et al., 2023; Zhao et al., 2014a). For example, while stem diameter variations within diverse communities can influence runoff (Mu et al., 2019; Zhao et al., 2016), this effect is complex and depends on vegetation density (Erktan et al., 2013; Yang et al., 2022). Similarly, the mixing of litter from different species can alter rainfall interception and redistribution characteristics (Han et al., 2024). Crucially, the recognized role of root systems in structuring soil is a key mechanism that was likely active in our experiment. Mixed plant root systems demonstrate superior hydrological performance compared to monocultures, with diverse root architectures (e.g., fibrous and tap roots) enhancing both saturated hydraulic conductivity and soil water content (Ma et al., 2024). Field studies of artificial grasslands further confirm that legume-grass mixtures, similar to those tested here, achieve higher soil infiltration capacity than monocultures through complementary below-ground biomass allocation (Wu et al., 2016). Depth stratification among species—ranging from shallow fibrous networks (0–10 cm) to deep taproots (>30 cm)—enhances profile-wide water storage and reduces surface sealing (Wu et al., 2016).

The relationship between species diversity and hydrological function was non-linear. Strong selection effects were evident, as the top-performing monoculture *Elymus dahuricus Turcz.* (ET) often outperformed low-diversity mixtures composed of specific legume-grass pairings (Cardinale et al., 2007). In contrast, the superior performance of the eight-species mixture suggests that complementarity effects became dominant. While we did not measure trait overlap, it is plausible that the success of the eight-species mixture stems from both functional complementarity and a degree of trait redundancy. Complementarity arises from niche differentiation in canopy architecture and root structure, which creates an emergent community function that surpasses that of any single species. Simultaneously, trait redundancy may provide an "insurance" effect, ensuring that key hydrological functions are maintained under stress thus enhancing overall ecosystem resilience (Chen et al., 2025).

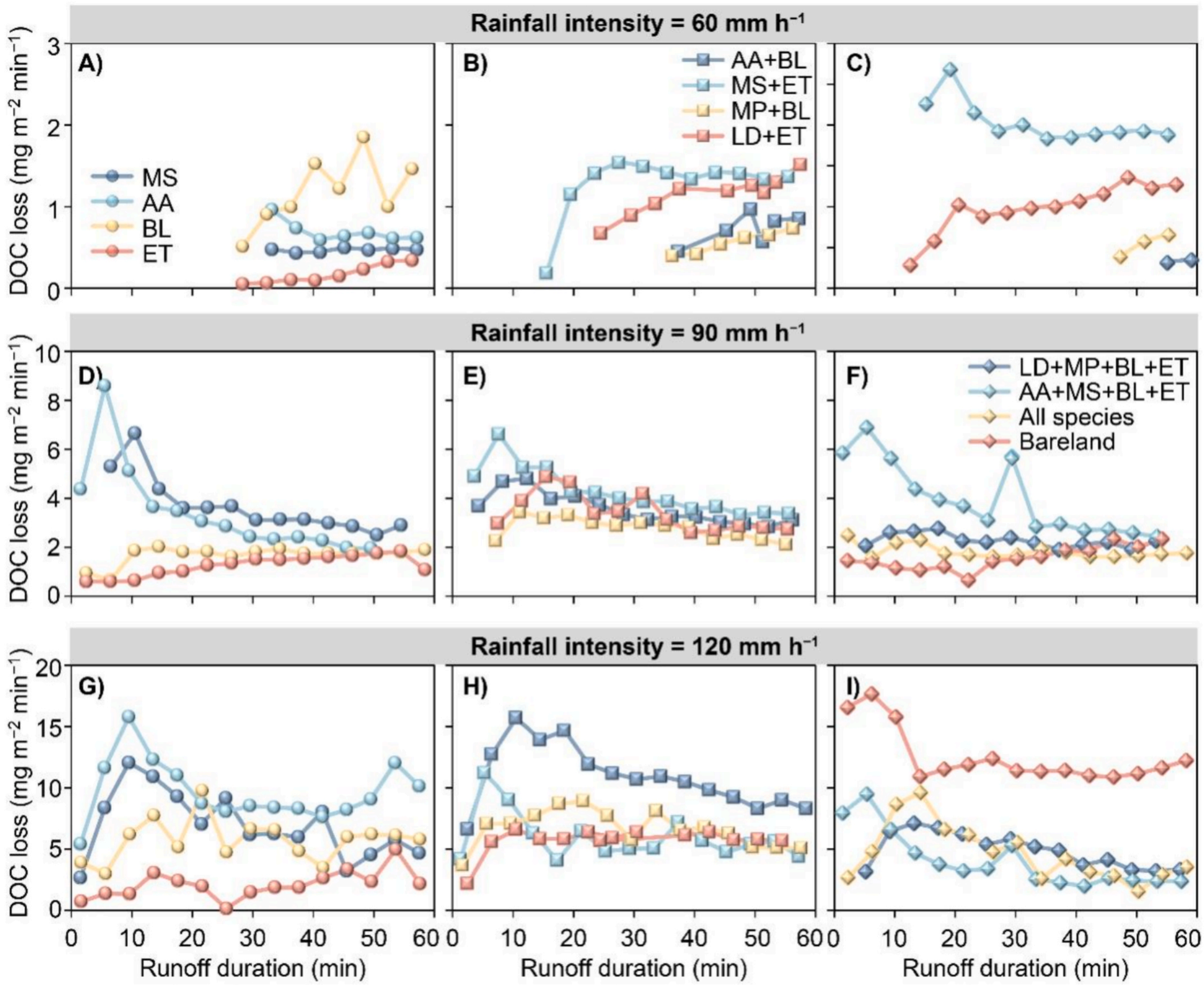

Fig. 5. Dissolved carbon loss rate processes under different species combined treatments and rainfall intensities. Dissolved carbon loss rate was measured for monocultures (A1, D, G), two-species mixtures (B, E, H), and multi-species mixtures including all species and bare land (C1, F, I) during simulated rainfall events at intensities of 60 mm h^{-1} (A–C), 90 mm h^{-1} (D–F), and 120 mm h^{-1} (G–I). MS, *Medicago sativa*; AA, *Astragalus adsurgens*; BL, *Bromus inermis*; ET, *Elymus dahuricus*; MP, *Melilotus officinalis*; LD, *Lespedeza daurica*.

4.2. The role of biodiversity in mitigating nutrient loss under extreme rainfall

Nutrient loss during slope runoff is influenced by multiple factors, including plant species, runoff volume, solute concentration and the exchange capacity between substrate and water flow (Shao et al., 2023; Sun et al., 2024; Wang et al., 2023). This study focused exclusively on DOC and DIN in runoff, omitting particulate-bound nutrients transported with sediment—a dominant pathway on the Loess Plateau, where sediment-bound organic carbon constitutes 87.5–99.6 % of total organic carbon loss in low-coverage systems (Hu et al., 2025; Sun et al., 2024; Li, 2019). Our results suggest that plant diversity mitigates dissolved nutrient loss primarily through its effects on runoff volume, GHD, and BDD. Contrary to the findings of Johnson et al. (2016), our study did not find that the effect of plant diversity on nutrient loss was mediated by biomass. This discrepancy may stem from the lack of a productivity advantage in our diverse plant communities. Kumari et al. (2024) and Silva et al. (2021) found that increasing crop species diversity reduces nutrient loss by enhancing land cover. Beyond biomass and cover, vegetation stratification enhances canopy interception and reduces leaching, thereby influencing nutrient loss in runoff (Wen et al., 2023). Wang et al. (2024) demonstrated that it is the hierarchical structure, rather than the leaf area index, that determines the loss of organic carbon. Additionally, plant diversity influences nutrient loss by affecting litterfall quantity and characteristics, which impacts runoff dynamics (Ouyang et al., 2022).

Vegetation effects on dissolved nutrient loss are modulated by rainfall characteristics, causing variations under different rainfall intensities (Muñoz et al., 2024). When rainfall intensity reached 120 mm h^{-1}, BDD became a significant influencing factor for slope runoff, TOC loss, and DIN loss, highlighting the contribution of near-surface resistance under extreme rainfall conditions (Mu et al., 2019). We observed that the impact of species mixtures on DOC and DIN loss varied with rainfall intensity. While two- and four-species mixtures increased dissolved nutrient loss at lower intensity (60 mm h^{-1}), this trend reversed at higher intensities (90 mm h^{-1} and 120 mm h^{-1}), suggesting a threshold effect. Specifically, our results indicate that mixtures of more than four species effectively reduced dissolved nutrient loss at 90 and 120-mm h^{-1} rainfall intensities. These findings are not consistent with those reported by Hunt et al. (2019) and Johnson et al. (2016). The

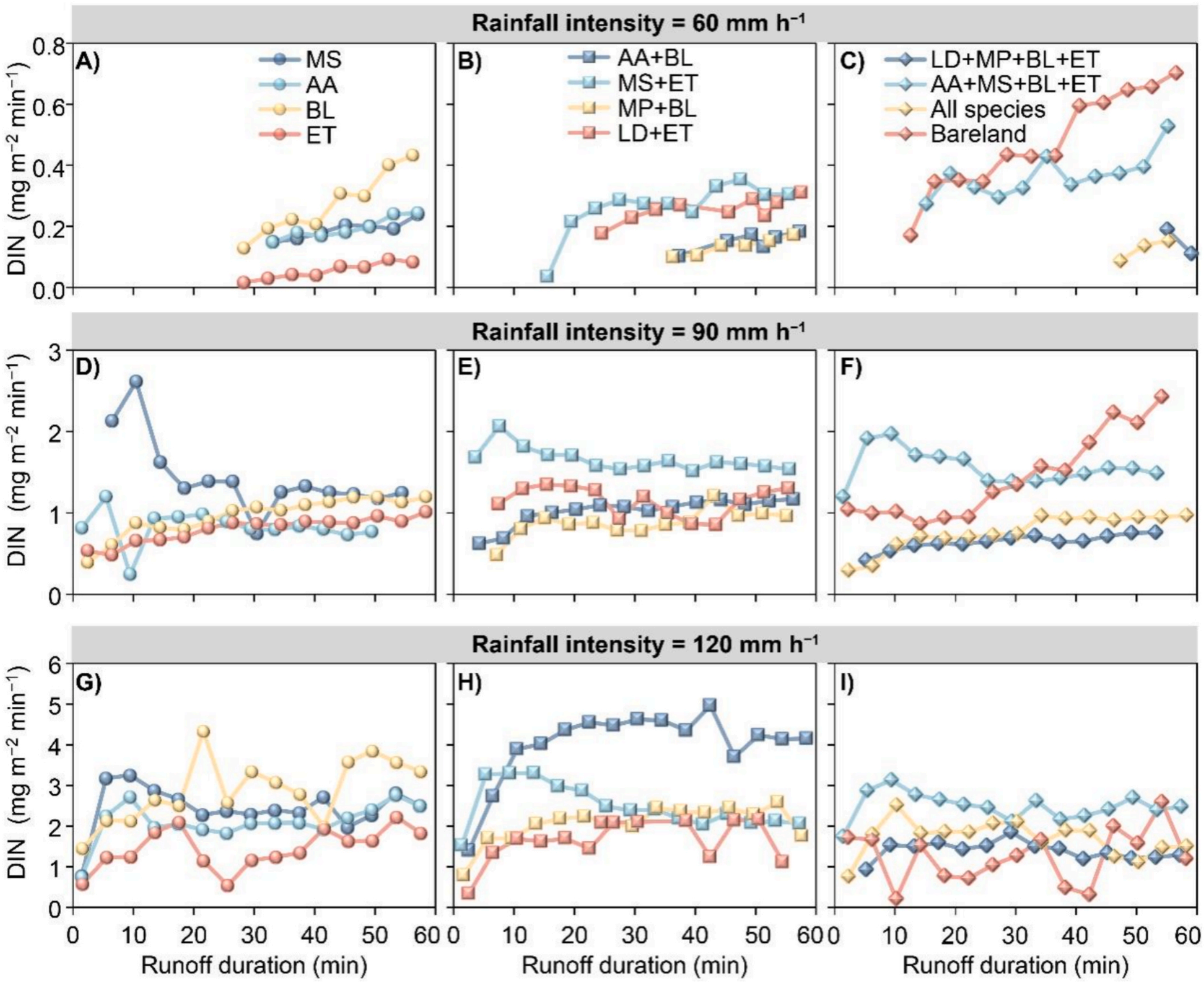

Fig. 6. Dissolved nitrogen loss rate processes under different species combined treatments and rainfall intensities. Ammonium nitrogen loss rate was measured for monocultures (A, D, G), two-species mixtures (B, E, H), and multi-species mixtures including all species and bare land (C, F, I) during simulated rainfall events at intensities of 60 mm h^{-1} (A–C), 90 mm h^{-1} (D–F), and 120 mm h^{-1} (G–I). MS, *Medicago sativa*; AA, *Astragalus adsurgens*; BL, *Bromus inermis*; ET, *Elymus dahuricus*; MP, *Melilotus officinalis*; LD, *Lespedeza daurica*.

relationship between runoff volume and nutrient concentration provides insights into nutrient transport mechanisms (Su et al., 2023). We found that DOC and DIN concentrations exhibited different patterns depending on rainfall intensities, they generally decreased with increasing runoff, suggesting a shift from transport limitation to source limitation (Moatar et al., 2017; Zarnetske et al., 2018). This could be attributed to the increase in raindrop kinetic energy with higher rainfall intensity (Zhu et al., 2023). At this point, the nutrient loss is constrained by the limited capacity of the soil surface exchange layer to transfer nutrients from the soil to the runoff (Li et al., 2017).

Due to negligible sediment yield in vegetated plots, insufficient particulate mass was collected for reliable sediment weight or bound-nutrient analysis—precluding quantification of sediment-bound carbon and nitrogen losses. This outcome reflects vegetation's erosion-control efficacy, Hu et al. (2025) reported that high coverage (>75%) reduces SOC loss by 96.2–99.9% relative to bare soil. As vegetation cover increases, the proportion of SOC loss decreases (from 99.4% in bare plots to 27.3% in vegetated plots), while DOC loss proportion rises (from 0.6% to 72.4%; Sun et al., 2024; Li, 2019). Thus, our dissolved-phase focus aligns with dominant nutrient pathways in restored grasslands, though particulate omissions may underestimate total fluxes.

4.3. Implications and limitations

The insights gained from this research can inform land management practices aimed at enhancing soil and water conservation in arid and semi-arid regions. By promoting plant diversity in grassland restoration and agricultural systems, stakeholders can effectively reduce soil erosion and nutrient loss, thereby improving ecosystem health and agricultural productivity (Chen et al., 2019, 2020; Feng et al., 2022; Gong et al., 2022). Policymakers and land managers should consider implementing biodiversity-enhancing strategies, such as mixed-species planting and the use of native grasses species (Wang et al., 2022; Wu et al., 2021), to bolster resilience against extreme weather events (Hong et al., 2022; Spohn et al., 2023), particularly extreme precipitation events. Extreme precipitation is a critical factor contributing to soil and water loss (Bian et al., 2023; Chang et al., 2023; Uber et al., 2024; Yan et al., 2024). Additionally, these findings can guide future research on the ecological benefits of biodiversity in various climatic contexts, contributing to the

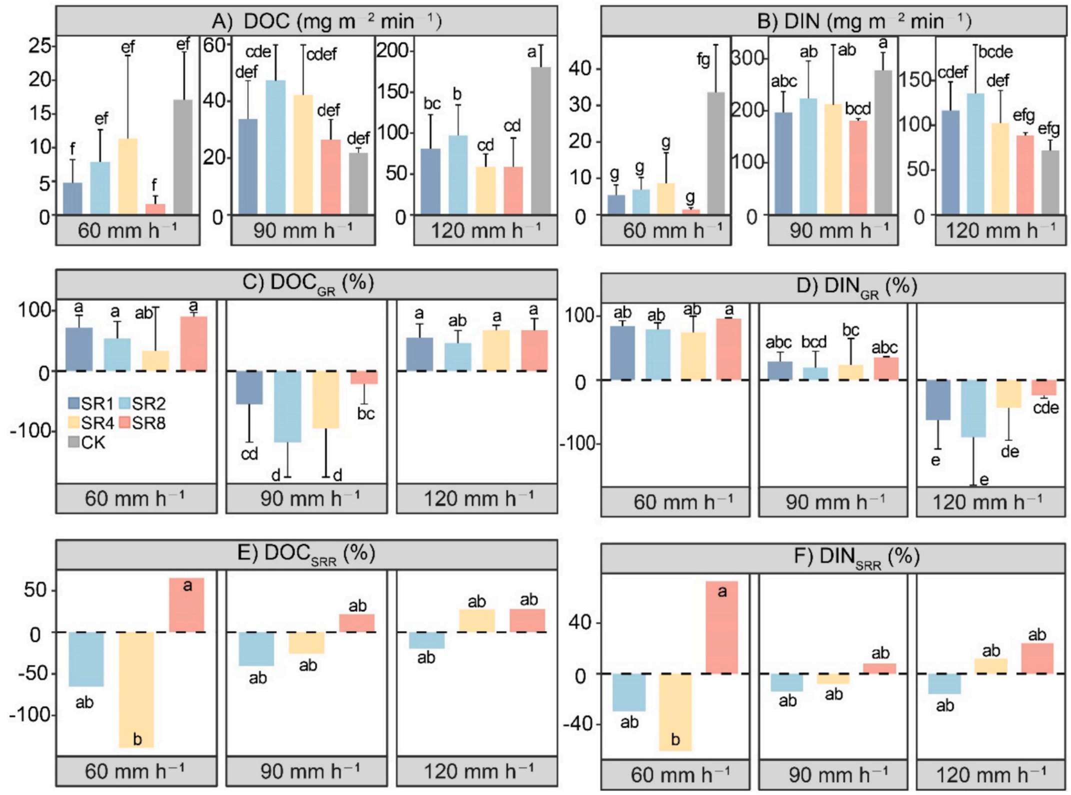

Fig. 7. The percentage reduction of total organic carbon (A, C, E) and total inorganic nitrogen (B, D, F) under different species richness and rainfall intensities. Different lowercase letters near error bars indicate a significant difference among rainfall intensities and species number at the $p < 0.05$ level.

development of adaptive management practices in the face of climate change.

While this study provides valuable insights into the role of plant diversity in mitigating runoff and nutrient loss, several limitations must be acknowledged. Primarily, our measurements were restricted to DOC and DIN in runoff, neglecting particulate-bound nutrients associated with sediment transport. This omission is significant on the Loess Plateau, where sediment-bound organic carbon can comprise up to 99.6 % of total losses in bare soils and remain substantial even under vegetation, potentially leading to underestimation of biodiversity's overall nutrient conservation benefits (Hu et al., 2025; Sun et al., 2024; Li, 2019). Consequently, conclusions regarding nutrient loss reductions apply solely to dissolved fractions and may not reflect total nutrient budgets. The controlled experimental conditions may not fully replicate the complexities of natural ecosystems, where multiple interacting factors influence hydrology and nutrient dynamics (Chen et al., 2023; Hagan et al., 2021; van der Plas, 2019). Furthermore, our study did not mechanistically disentangle the effects of functional complementarity from trait redundancy. Without direct measurements of key belowground traits like root depth and architecture, our capacity to attribute the observed benefits to specific trait interactions is constrained. The uniform, broadcast sowing method also does not account for the influence of fine-scale spatial plant configurations, which can significantly affect ecohydrological processes. The focus on specific grass species may limit the generalizability of the findings to other plant communities or ecosystems (Dee et al., 2023; Zheng et al., 2024). Additionally, our single time-point measurements after simulated rainfall fail to capture the potential legacy effects of biodiversity on soil recovery. A single-event design cannot assess whether diverse communities sustain higher infiltration rates or exhibit faster pore-structure regeneration in subsequent rainfall events. Future research should explore the long-term effects of biodiversity on soil and water conservation in diverse environmental contexts and consider the interactions between plant diversity and other ecological factors, such as soil health and microbial communities (Domeignoz-Horta et al., 2024; Lange et al., 2023; Zhou et al., 2024). Furthermore, the study's reliance on simulated rainfall may not capture the full range of variability present in natural precipitation events, necessitating further field studies to validate the results (Carvalho et al., 2022; Meena et al., 2022; Menezes Sanchez Macedo et al., 2021).

5. Conclusion

Our findings establish species diversity in grassland communities as a fundamental driver of ecosystem hydrological resilience. The demonstrated capacity of eight-species assemblages to reduce runoff by up to 93.76% and nutrient losses by >90% reveals biodiversity as a quantifiable engineering parameter for nature-based solutions. Mechanistically, this research advances the understanding of diversity-function relationships under climate stress. Grass height diversity emerged as the dominant structural control across rainfall intensities, superseding traditional biomass-based models and highlighting canopy architecture as the primary design criterion for resilient grassland systems. The intensity-dependent shift in control from biomass to basal diameter diversity demonstrates an adaptive community-level response under extreme precipitation—a critical insight for climate-proofing restoration strategies. Furthermore, the benefits of diversity are non-linear and contingent on complementarity. The frequent underperformance of two-species mixtures compared to top-performing monocultures underscores the risk of relying on simple mixtures where negative interactions or a lack of functional complementarity can undermine ecosystem services. These findings provide a clear directive for land management and ecological restoration. Instead of focusing solely on species counts, management strategies should prioritize the selection of species with complementary functional traits that enhance canopy stratification and root system diversity.

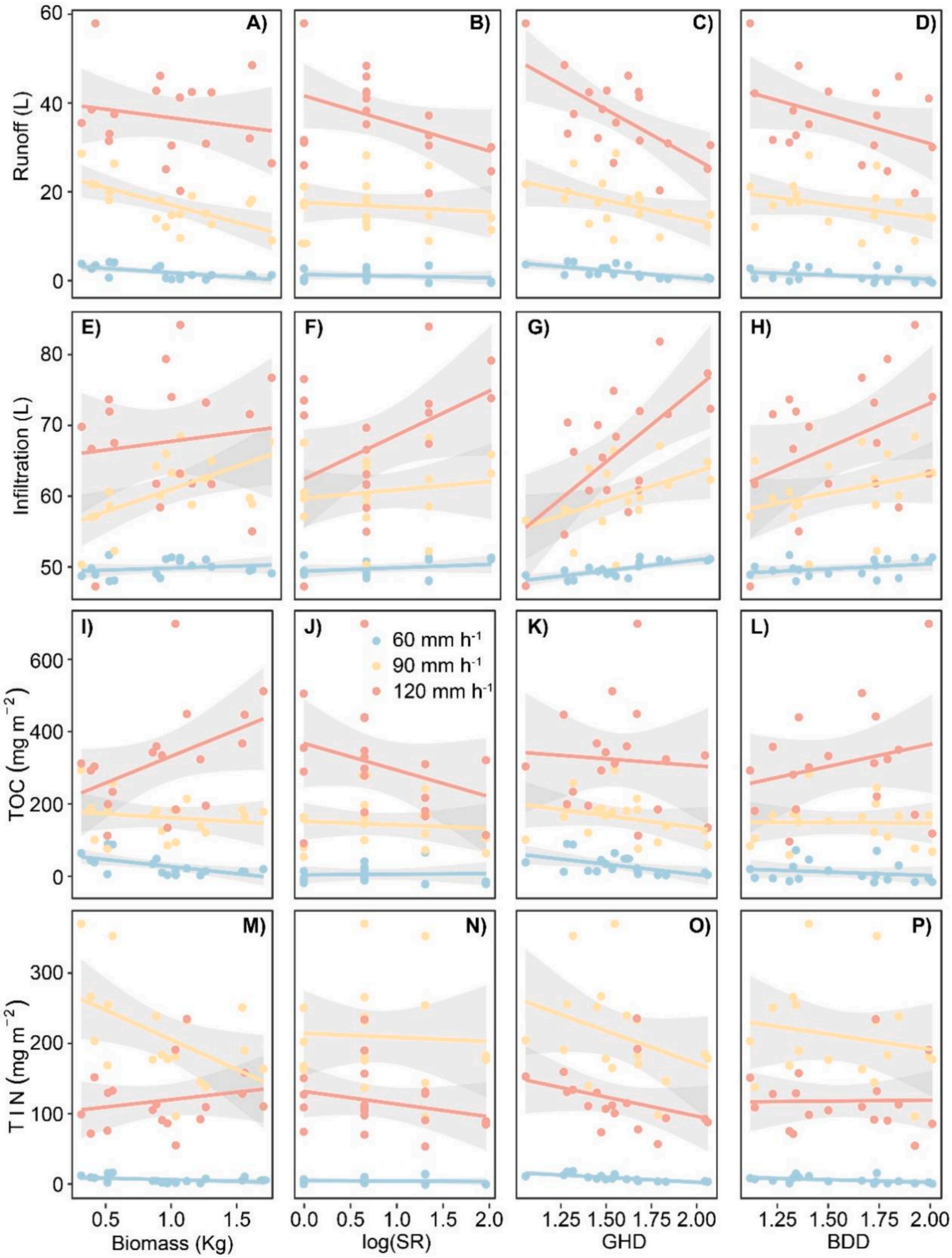

Fig. 8. Relationship between plant traits and total runoff and infiltration. A) Relationship between biomass and runoff. B) Relationship between species richness (SR) and runoff. C) Relationship between grass height diversity (GHD) and runoff. D) Relationship between basal diameter diversity (BDD) and runoff. E) Relationship between biomass and infiltration. F) Relationship between SR and infiltration. G) Relationship between GHD and infiltration. H) Relationship between BDD and Infiltration. I) Relationship between biomass and total dissolved organic carbon loss (TOC). J) Relationship between SR and TOC. K) Relationship between GHD and runoff. L) Relationship between BDD and runoff. M) Relationship between biomass and total dissolved inorganic nitrogen loss (DIN). N) Relationship between SR and DIN. O) Relationship between GHD and DIN. P) Relationship between BDD and DIN. Coefficients of determination R^2 and *p*-values shown in Supplement Table.

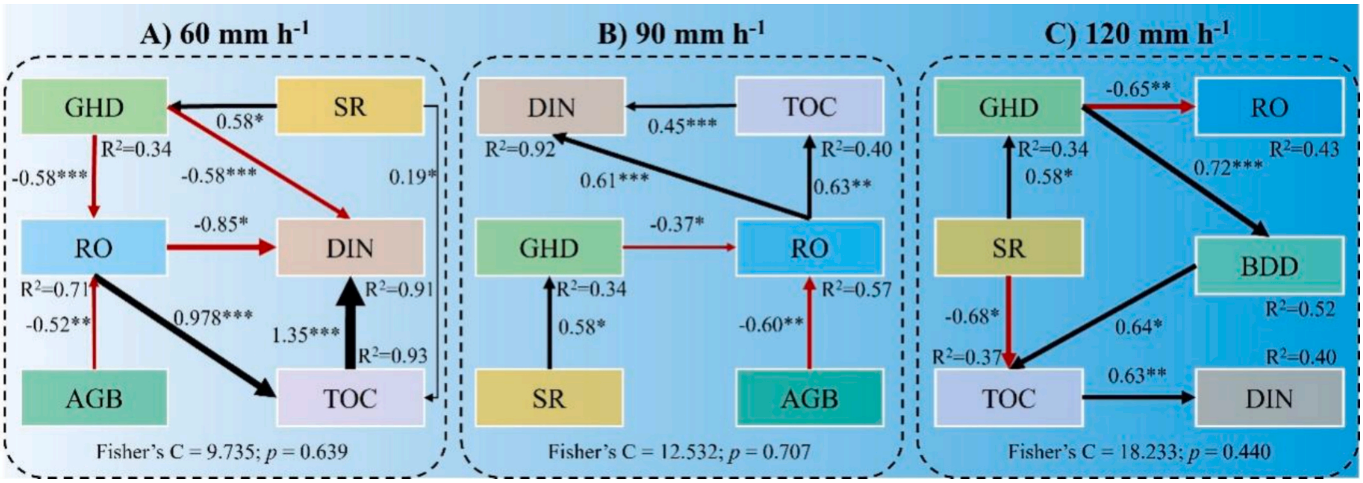

Fig. 9. Piecewise structural equation modelling analysis of plant traits on runoff (RO), total dissolved organic carbon loss (loss) and total dissolved inorganic nitrogen loss (DIN). Species richness (SR), plant aboveground biomass (AGB), grass height diversity (GHD) and basal diameter diversity (BDD). A) 60 mm h^{-1}, B) 90 mm h^{-1}, C)120 mm h^{-1}. Note: The numbers inscribed on the lines correspond to the normalized path coefficients. Path thickness reflects standardized model coefficients. * $p < 0.05$; ** $p < 0.01$; *** $p < 0.001$.

CRediT authorship contribution statement

Huaqing Liu: Writing – original draft, Visualization, Methodology, Formal analysis, Data curation. **Yaohui Cai:** Writing – review & editing, Supervision, Conceptualization. **Xiaodong Gao:** Writing – review & editing, Visualization, Conceptualization. **Long Ma:** Data curation. **Heng Liu:** Data curation. **Xining Zhao:** Writing – review & editing, Supervision, Funding acquisition.

Declaration of competing interest

The authors declare that they have no known competing financial interests or personal relationships that could have appeared to influence the work reported in this paper.

Acknowledgements

This research was funded by the National Natural Science Foundation of China (U22A20613), the National Key Research and Development Program of China (2021YFD1900700), the Key Research and Development Program of Shaanxi Province (2023-ZDLNY-49), the Natural Science Basic Research Program of Shaanxi Province (2023JC-XJ-24), the Central Government Guidance Funds for Local Science and Technology Development (2024ZY-JCYJ-02-27).

Appendix A. Supplementary data

Supplementary data to this article can be found online at https://doi.org/10.1016/j.jhydrol.2025.134499.

Data availability

Data will be made available on request.

References

Allen, D.C., Cardinale, B.J., Wynn-Thompson, T., 2016. Plant biodiversity effects in reducing fluvial erosion are limited to low species richness. Ecology 97, 17–24. https://doi.org/10.1890/15-0800.1.

Barry, K.E., Mommer, L., van Ruijven, J., Wirth, C., Wright, A.J., Bai, Y., Connolly, J., De Deyn, G.B., de Kroon, H., Isbell, F., Milcu, A., Roscher, C., Scherer-Lorenzen, M., Schmid, B., Weigelt, A., 2019. The future of complementarity: disentangling causes from consequences. Trends Ecol. Evol. 34, 167–180. https://doi.org/10.1016/j.tree.2018.10.013.

Berendse, F., van Ruijven, J., Jongejans, E., Keesstra, S., 2015. Loss of plant species diversity reduces soil erosion resistance. Ecosystems 18, 881–888. https://doi.org/10.1007/s10021-015-9869-6.

Bian, Z., Sun, G., McNulty, S., Pan, S., Tian, H., 2023. Understanding the shift of drivers of soil erosion and sedimentation based on regional process-based modeling in the Mississippi river basin during the past century. Water Resour. Res. 59, e2023WR035377. https://doi.org/10.1029/2023WR035377.

Borrelli, P., Robinson, D.A., Fleischer, L.R., Lugato, E., Ballabio, C., Alewell, C., Meusburger, K., Modugno, S., Schütt, B., Ferro, V., Bagarello, V., Oost, K.V., Montanarella, L., Panagos, P., 2017. An assessment of the global impact of 21st century land use change on soil erosion. Nat. Commun. 8, 2013. https://doi.org/10.1038/s41467-017-02142-7.

Cardinale, B.J., Wright, J.P., Cadotte, M.W., Carroll, I.T., Hector, A., Srivastava, D.S., Loreau, M., Weis, J.J., 2007. Impacts of plant diversity on biomass production increase through time because of species complementarity. PNAS 104, 18123–18128. https://doi.org/10.1073/pnas.0709069104.

Carvalho, D.F.de, Macedo, P.M.S., Pinto, M.F., de Almeida, W.S., Schultz, N., 2022. Soil loss and runoff obtained with customized precipitation patterns simulated by InfiAsper. Int. Soil Water Conserv. Res. 10, 407–413. https://doi.org/10.1016/j.iswcr.2021.12.003.

Chang, D., Li, S., Lai, Z., 2023. Effects of extreme precipitation intensity and duration on the runoff and nutrient yields. J. Hydrol. 626, 130281. https://doi.org/10.1016/j.jhydrol.2023.130281.

Chen, C., Chen, H.Y.H., Chen, X., Huang, Z., 2019. Meta-analysis shows positive effects of plant diversity on microbial biomass and respiration. Nat. Commun. 10, 1332. https://doi.org/10.1038/s41467-019-09258-y.

Chen, C., Xiao, W., Chen, H.Y.H., 2025. Meta-analysis reveals global variations in plant diversity effects on productivity. Nature 638, 435–440. https://doi.org/10.1038/s41586-024-08407-8.

Chen, X., Chen, H.Y.H., Chen, C., Ma, Z., Searle, E.B., Yu, Z., Huang, Z., 2020. Effects of plant diversity on soil carbon in diverse ecosystems: a global meta-analysis. Biol. Rev. 95, 167–183. https://doi.org/10.1111/brv.12554.

Chen, X., Taylor, A.R., Reich, P.B., Hisano, M., Chen, H.Y.H., Chang, S.X., 2023. Tree diversity increases decadal forest soil carbon and nitrogen accrual. Nature 618, 94–101. https://doi.org/10.1038/s41586-023-05941-9.

Dee, L.E., Ferraro, P.J., Severen, C.N., Kimmel, K.A., Borer, E.T., Byrnes, J.E.K., Clark, A.T., Hautier, Y., Hector, A., Raynaud, X., Reich, P.B., Wright, A.J., Arnillas, C.A., Davies, K.F., MacDougall, A., Mori, A.S., Smith, M.D., Adler, P.B., Bakker, J.D., Brauman, K.A., Cowles, J., Komatsu, K., Knops, J.M.H., McCulley, R.L., Moore, J.L., Morgan, J.W., Ohlert, T., Power, S.A., Sullivan, L.L., Stevens, C., Loreau, M., 2023. Clarifying the effect of biodiversity on productivity in natural ecosystems with longitudinal data and methods for causal inference. Nat. Commun. 14, 2607. https://doi.org/10.1038/s41467-023-37194-5.

Domeignoz-Horta, L.A., Cappelli, S.L., Shrestha, R., Gerin, S., Lohila, A.K., Heinonsalo, J., Nelson, D.B., Kahmen, A., Duan, P., Sebag, D., Verrecchia, E., Laine, A.-L., 2024. Plant diversity drives positive microbial associations in the rhizosphere enhancing carbon use efficiency in agricultural soils. Nat. Commun. 15, 8065. https://doi.org/10.1038/s41467-024-52449-5.

Dong, Y., Lei, T., Li, S., Yuan, C., Zhou, S., Yang, X., 2015. Effects of rye grass coverage on soil loss from loess slopes. Int. Soil Water Conserv. Res. 3, 170–182. https://doi.org/10.1016/j.iswcr.2015.05.006.

Eisenhauer, N., 2022. The shape that matters: how important is biodiversity for ecosystem functioning? Sci. China Life Sci. 65, 651–653. https://doi.org/10.1007/s11427-021-2052-5.

Erktan, A., Cécillon, L., Roose, E., Frascaria-Lacoste, N., Rey, F., 2013. Morphological diversity of plant barriers does not increase sediment retention in eroded marly

gullies under ecological restoration. Plant and Soil 370, 653–669. https://doi.org/10.1007/s11104-013-1738-5.
Feng, Y., Schmid, B., Loreau, M., Forrester, D.I., Fei, S., Zhu, J., Tang, Z., Zhu, J., Hong, P., Ji, C., Shi, Y., Su, H., Xiong, X., Xiao, J., Wang, S., Fang, J., 2022. Multispecies forest plantations outyield monocultures across a broad range of conditions. Science 376, 865–868. https://doi.org/10.1126/science.abm6363.
Geißler, C., Kühn, P., Böhnke, M., Bruelheide, H., Shi, X., Scholten, T., 2012. Splash erosion potential under tree canopies in subtropical SE china. Catena 91, 85–93. https://doi.org/10.1016/j.catena.2010.10.009.
Gong, C., Tan, Q., Liu, G., Xu, M., 2022. Impacts of mixed forests on controlling soil erosion in China. Catena 213, 106147. https://doi.org/10.1016/j.catena.2022.106147.
Hagan, J., Vanschoenwinkel, B., Gamfeldt, L., 2021. We should not necessarily expect positive relationships between biodiversity and ecosystem functioning in observational field data. Ecol. Lett. 24, 2537–2548. https://doi.org/10.1111/ele.13874.
Han, Z., Li, K., Fang, Q., Fan, C., Zhao, L., 2024. Rainfall interception by leaf litters: what happens with fallen leaves of different types and mixing degrees under simulated rainfall? J. Hydrol. 637, 131390. https://doi.org/10.1016/j.jhydrol.2024.131390.
He, Q., Li, B., Zhang, F., Shen, N., Yang, M., 2024. Runoff and Infiltration responses of revegetated slopes to clipping management on the northern Loess Plateau. Int. Soil Water Conserv. Res. 12, 171–183. https://doi.org/10.1016/j.iswcr.2023.02.004.
Hector, A., Bagchi, R., 2007. Biodiversity and ecosystem multifunctionality. Nature 448, 188–190. https://doi.org/10.1038/nature05947.
Hong, P., Schmid, B., De Laender, F., Eisenhauer, N., Zhang, X., Chen, H., Craven, D., De Boeck, H.J., Hautier, Y., Petchey, O.L., Reich, P.B., Steudel, B., Striebel, M., Thakur, M.P., Wang, S., 2022. Biodiversity promotes ecosystem functioning despite environmental change. Ecol. Lett. 25, 555–569. https://doi.org/10.1111/ele.13936.
Hu, X., Li, Y., Guo, W., Li, J., Zhu, X., Luo, L., Tian, P., Sun, H., 2025. Inhibiting effects of vegetation coverage on runoff, sediment, and organic carbon loss on steep loess gully-slopes. Land Degrad. Dev. https://doi.org/10.1002/ldr.70039.
Hunt, N.D., Hill, J.D., Liebman, M., 2019. Cropping system diversity effects on nutrient discharge, soil erosion, and agronomic performance. Environ. Sci. Technol. 53, 1344–1352. https://doi.org/10.1021/acs.est.8b02193.
Hurtado, P., Aragón, G., Vicente, M., Dalsgaard, B., Krasnov, B.R., Calatayud, J., 2024. Generalism in species interactions is more the consequence than the cause of ecological success. Nat. Ecol. Evol. 8, 1602–1611. https://doi.org/10.1038/s41559-024-02484-8.
Jiang, S., Wang, L., Shu, H., Li, S., Yang, J., 2024. "cutting effect" of needles on the raindrop characteristics. J. Hydrol. 631, 130783. https://doi.org/10.1016/j.jhydrol.2024.130783.
Johnson, C., Schweinhart, S., Buffam, I., 2016. Plant species richness enhances nitrogen retention in green roof plots. Ecol. Appl. 26, 2130–2144. https://doi.org/10.1890/15-1850.1.
Kassambara, A., 2023. ggpubr: "ggplot2" Based Publication Ready Plots.
Kervroëdan, L., Armand, R., Saunier, M., Faucon, M.-P., 2020. Functional diversity effects of vegetation on runoff to design herbaceous hedges for sediment retention. Australas. i. Min. Met. 12, 131. https://doi.org/10.3390/d12040131.
Kumari, V.V., Balloli, S.S., Kumar, M., Ramana, D.B.V., Prabhakar, M., Osman, M., Indoria, A.K., Manjunath, M., Maruthi, V., Chary, G.R., Chandran, M.A.S., Gopinath, K.A., Venkatesh, G., Rao, M.S., Singh, V.K., Timsina, J., 2024. Diversified cropping systems for reducing soil erosion and nutrient loss and for increasing crop productivity and profitability in rainfed environments. Agric. Syst. 217, 103919. https://doi.org/10.1016/j.agsy.2024.103919.
Lange, M., Eisenhauer, N., Chen, H., Gleixner, G., 2023. Increased soil carbon storage through plant diversity strengthens with time and extends into the subsoil. Glob. Chang. Biol. 29, 2627–2639. https://doi.org/10.1111/gcb.16641.
Laws, J.O., 1941. Measurements of the fall-velocity of water -drops and raindrops. Eos Trans. AGU 22, 709–721. https://doi.org/10.1029/TR022i003p00709.
Lees, C., de Baets, S., Rickson, J., Simmons, R.W., 2021. Selecting plant traits for soil erosion control in grassed waterways under a changing climate: a growth room study. Eur. J. Soil Sci. 72, 2381–2397. https://doi.org/10.1111/ejss.13045.
Lefcheck, J.S., 2016. piecewiseSEM: piecewise structural equation modelling in r for ecology, evolution, and systematics. Methods Ecol. Evol. 7, 573–579. https://doi.org/10.1111/2041-210X.12512.
Li, J., 2019. The Effect of Vegetation Restoration on Soil Carbon Dynamics During Rainfall-Erosion Processes in an Eroding Landscape on the Loess Plateau. University of Chinese Academy of Sciences, Beijing.
Li, J., Li, L., Wang, W., Kang, H., Guo, M., Huang, J., Wang, Y., Lou, Y., Tong, X., Nie, H., 2023. Hydrological and erosion responses of steep spoil heaps to taproot and fibrous root grasses under simulated rainfalls. J. Hydrol. 618, 129169. https://doi.org/10.1016/j.jhydrol.2023.129169.
Li, J., Tong, J., Xia, C., Hu, B.X., Zhu, H., Yang, R., Wei, W., 2017. Numerical simulation and experimental study on farmland nitrogen loss to surface runoff in a raindrop driven process. J. Hydrol. 549, 754–768. https://doi.org/10.1016/j.jhydrol.2017.01.035.
Liu, C., Zhang, K., Wei, S., Wang, P., Cen, Y., Xia, J., 2023. Evaluation of the effects of grass and shrub cover on overland flow resistance and its attributes under simulated rainfall. J. Hydrol. 626, 130285. https://doi.org/10.1016/j.jhydrol.2023.130285.
Liu, H., Gao, X., Li, C., Cai, Y., Song, X., Zhao, X., 2025a. Intercropping increases plant water availability and water use efficiency: a synthesis. Agric. Ecosyst. Environ. 379, 109360. https://doi.org/10.1016/j.agee.2024.109360.
Liu, H., Gao, X., Li, C., Ma, L., Siddique, K.H.M., Zhao, X., 2024. Short-term plant mixtures alter soil organic carbon components and microbial network characteristics. Eur. J. Soil Biol. 122, 103650. https://doi.org/10.1016/j.ejsobi.2024.103650.
Liu, H., Yang, J., Liu, C., Diao, Y., Ma, D., Li, F., Rahma, A.E., Lei, T., 2020a. Flow velocity on cultivated soil slope with wheat straw incorporation. J. Hydrol. 584, 124667. https://doi.org/10.1016/j.jhydrol.2020.124667.
Liu, H., Gao, X., Ma, L., Liu, H., Zhao, X., 2025b. Herbaceous species richness enhances soil hydraulic conductivity by increasing soil pore connectivity. J. Hydrol. 663, 134218. https://doi.org/10.1016/j.jhydrol.2025.134218.
Liu, H., Gao, X., Zhao, X., 2025c. Scale-dependent effects of tree species diversity on soil erosion resistance. Resour. Environ. Sustain. 21, 100221. https://doi.org/10.1016/j.resenv.2025.100221.
Liu, Y., Dunkerley, D., López-Vicente, M., Shi, Z., Wu, G., 2020b. Trade-off between surface runoff and soil erosion during the implementation of ecological restoration programs in semiarid regions: a meta-analysis. Sci. Total Environ. 712, 136477. https://doi.org/10.1016/j.scitotenv.2019.136477.
Liu, Y., Li, S., Shi, J., Niu, Y., Cui, Z., Zhang, Z., Wang, Y., Ma, Y., López-Vicente, M., Wu, G.-L., 2022a. Effectiveness of mixed cultivated grasslands to reduce sediment concentration in runoff on hillslopes in the Qinghai-Tibetan plateau. Geoderma 422, 115933. https://doi.org/10.1016/j.geoderma.2022.115933.
Liu, Y., Huang, Z., Meng, L., Li, S., Wang, Y., Liu, Yu., López-vicente, M., Wu, G., 2022b. Understory shading exacerbated grassland soil erosion by changing community composition. Catena 208, 105771. https://doi.org/10.1016/j.catena.2021.105771.
Ma, J., Li, Z., Li, P., Ma, B., Xiao, L., Cui, Z., Wang, Z., Min, Z., 2024. Effect of mixed plant roots on saturated hydraulic conductivity and saturated water content of soil in the loess region. Agric. Water Manage. 295, 108784. https://doi.org/10.1016/j.agwat.2024.108784.
Ma, J., Ma, B., Li, Z., Wang, C., Shang, Y., Zhang, Z., 2023. Determining the mechanism of the root effect on soil detachment under mixed modes of different plant species using flume simulation. Sci. Total Environ. 858, 159888. https://doi.org/10.1016/j.scitotenv.2022.159888.
Martin, C., Pohl, M., Alewell, C., Körner, C., Rixen, C., 2010. Interrill erosion at disturbed alpine sites: effects of plant functional diversity and vegetation cover. Basic Appl. Ecol. 11, 619–626. https://doi.org/10.1016/j.baae.2010.04.006.
Meena, R.K., Sen, S., Nanda, A., Dass, B., Mishra, A., 2022. A contribution to rainfall simulator design – a concept of moving storm automation. Hydrol. Earth Syst. Sci. 26, 4379–4390. https://doi.org/10.5194/hess-26-4379-2022.
Mendiburu, F. de, 2023. agricolae: Statistical Procedures for Agricultural Research.
Menezes Sanchez, P., Ferreira Pinto, M., Alves Sobrinho, T., Schultz, N., Altamir Rodrigues Coutinho, T., Fonseca de Carvalho, D., 2021. A modified portable rainfall simulator for soil erosion assessment under different rainfall patterns. J. Hydrol. 596, 126052. https://doi.org/10.1016/j.jhydrol.2021.126052.
Moatar, F., Abbott, B.W., Minaudo, C., Curie, F., Pinay, G., 2017. Elemental properties, hydrology, and biology interact to shape concentration-discharge curves for carbon, nutrients, sediment, and major ions. Water Resour. Res. 53, 1270–1287. https://doi.org/10.1002/2016WR019635.
Mu, H., Yu, X., Fu, S., Yu, B., Liu, Y., Zhang, G., 2019. Effect of stem cover on hydraulic parameters of overland flow. J. Hydrol. 577, 123964. https://doi.org/10.1016/j.jhydrol.2019.123964.
Muñoz, J.A., Guzmán, G., Soriano, M.A., Gómez, J.A., 2024. Appraising trapping efficiency of vegetative barriers in agricultural landscapes: Strategy based on a probabilistic approach based on a review of available information. Int. Soil Water Conserv. Res. 12, 615–634. https://doi.org/10.1016/j.iswcr.2023.12.001.
Nanko, K., Mizugaki, S., Onda, Y., 2008. Estimation of soil splash detachment rates on the forest floor of an unmanaged Japanese cypress plantation based on field measurements of throughfall drop sizes and velocities. Catena 72, 348–361. https://doi.org/10.1016/j.catena.2007.07.002.
Ouyang, W., Wu, Z., Wang, P., Cui, X., Hao, X., Zhu, W., Jin, R., 2022. Diffuse nutrient export dynamics from accumulated litterfall in forested watersheds with remote sensing data coupled model. Water Res. 209, 117948. https://doi.org/10.1016/j.watres.2021.117948.
Panagos, P., Borrelli, P., Matthews, F., Liakos, L., Bezak, N., Diodato, N., Ballabio, C., 2022. Global rainfall erosivity projections for 2050 and 2070. J. Hydrol. 610, 127865. https://doi.org/10.1016/j.jhydrol.2022.127865.
R Core Team, 2023. R: A language and environment for statistical computing.
Shang, H., Zhang, K., Wang, Z., Yang, J., He, M., Pan, X., Fang, C., 2020. Effect of varying wheatgrass density on resistance to overland flow. J. Hydrol. 591, 125594. https://doi.org/10.1016/j.jhydrol.2020.125594.
Shao, F., Tao, W., Wang, Q., Wu, J., Su, L., Yan, H., Zhang, Y., 2023. A mathematical model using an equivalent exchange layer for predicting raindrop-induced nutrient ejection from soil to runoff on bare and vegetated slopes. J. Hydrol. 620, 129546. https://doi.org/10.1016/j.jhydrol.2023.129546.
Shi, X., Lei, T., Zhang, F., Yan, Y., 2015. Velocity measurement of water flow within gravel layer with electrolyte tracer method under virtual boundary condition. J. Hydrol. 527, 387–393. https://doi.org/10.1016/j.jhydrol.2015.05.008.
Silva, L.de C.M. da, Avanzi, J.C., Peixoto, D.S., Merlo, M.N., Borghi, E., de Resende, Á.V., Acuña-Guzman, S.F., Silva, B.M., 2021. Ecological intensification of cropping systems enhances soil functions, mitigates soil erosion, and promotes crop resilience to dry spells in the Brazilian Cerrado. Int. Soil Water Conserv. Res. 9, 591–604. https://doi.org/10.1016/j.iswcr.2021.06.006.
Spohn, M., Bagchi, S., Biederman, L.A., Borer, E.T., Bråthen, K.A., Bugalho, M.N., Caldeira, M.C., Catford, J.A., Collins, S.L., Eisenhauer, N., Hagenah, N., Haider, S., Hautier, Y., Knops, J.M.H., Koerner, S.E., Laanisto, L., Lekberg, Y., Martina, J.P., Martinson, H., McCulley, R.L., Peri, P.L., Macek, P., Power, S.A., Risch, A.C., Roscher, C., Seabloom, E.W., Stevens, C., Veen, G.F., Virtanen, R., Yahdjian, L., 2023. The positive effect of plant diversity on soil carbon depends on climate. Nat. Commun. 14, 6624. https://doi.org/10.1038/s41467-023-42340-0.
Su, H., Cheng, L., Wu, Y., Qin, S., Liu, P., Zhang, Q., Cheng, S., Li, Y., 2023. Extreme storm events shift DOC export from transport-limited to source-limited in a typical

flash flood catchment. J. Hydrol. 620, 129377. https://doi.org/10.1016/j.jhydrol.2023.129377.
Sun, H., Luo, L., Guo, W., Hu, X., Xu, Y., Wang, W., 2024. Exploring rational vegetation configuration to relative increase runoff, reduce erosion and soil organic carbon loss in gully-slopes on the Chinese Loess Plateau. J. Hydrol. 640, 131678. https://doi.org/10.1016/j.jhydrol.2024.131678.
Tilman, D., 2000. Causes, consequences and ethics of biodiversity. Nature 405, 208–211. https://doi.org/10.1038/35012217.
Uber, M., Haller, M., Brendel, C., Hillebrand, G., Hoffmann, T., 2024. Past, present and future rainfall erosivity in central Europe based on convection-permitting climate simulations. Hydrol. Earth Syst. Sci. 28, 87–102. https://doi.org/10.5194/hess-28-87-2024.
van der Plas, F., 2019. Biodiversity and ecosystem functioning in naturally assembled communities. Biol. Rev. 94, 1220–1245. https://doi.org/10.1111/brv.12499.
Wang, C., Zhang, W., Li, X., Wu, J., 2022. A global meta-analysis of the impacts of tree plantations on biodiversity. Glob. Ecol. Biogeogr. 31, 576–587. https://doi.org/10.1111/geb.13440.
Wang, H., Zhang, Q., Li, X., Yi, Y., Wang, Q., Gao, L., Wang, J., He, D., Li, M., 2023. Surface microrelief induced by tillage management alters the pathway and composition of dissolved organic matter exports from soils to runoff during rainfall. Water Res. 245, 120554. https://doi.org/10.1016/j.watres.2023.120554.
Wang, W., Xu, C., Lin, T.-C., Yang, Z., Liu, X., Xiong, D., Chen, S., Chen, G., Yang, Y., 2024. Forest structure regulates response of erosion-induced carbon loss to rainfall characteristics. Forests 15, 1269. https://doi.org/10.3390/f15071269.
Weisser, W.W., Roscher, C., Meyer, S.T., Ebeling, A., Luo, G., Allan, E., Beßler, H., Barnard, R.L., Buchmann, N., Buscot, F., Engels, C., Fischer, C., Fischer, M., Gessler, A., Gleixner, G., Halle, S., Hildebrandt, A., Hillebrand, H., De Kroon, H., Lange, M., Leimer, S., Le Roux, X., Milcu, A., Mommer, L., Niklaus, P.A., Oelmann, Y., Proulx, R., Roy, J., Scherber, C., Scherer-Lorenzen, M., Scheu, S., Tscharntke, T., Wachendorf, M., Wagg, C., Weigelt, A., Wilcke, W., Wirth, C., Schulze, E.-D., Schmid, B., Eisenhauer, N., 2017. Biodiversity effects on ecosystem functioning in a 15-year grassland experiment: patterns, mechanisms, and open questions. Basic Appl. Ecol. 23, 1–73. https://doi.org/10.1016/j.baae.2017.06.002.
Wen, B., Duan, G., Lu, J., Zhou, R., Ren, H., Wen, Z., 2023. Response relationship between vegetation structure and runoff-sediment yield in the hilly and gully area of the Loess Plateau, China. Catena 227, 107107. https://doi.org/10.1016/j.catena.2023.107107.
Wen, Z., Zheng, H., Zhao, H., Liu, L., Ouyang, Z., 2021. Species compositional, structural and functional diversity exerts different effects on soil erosion caused by increased rainfall intensity in Chinese tropical forests. Plant Soil 465, 97–108. https://doi.org/10.1007/s11104-021-04980-3.
Wu, G., Liu, Y., Cui, Z., Liu, Yu., Shi, Z., Yin, R., Kardol, P., 2020. Trade-off between vegetation type, soil erosion control and surface water in global semi-arid regions: a meta-analysis. J. Appl. Ecol. 57, 875–885. https://doi.org/10.1111/1365-2664.13597.
Wu, G., Yang, Z., Cui, Z., Liu, Y., Fang, N., Shi, Z., 2016. Mixed artificial grasslands with more roots improved mine soil infiltration capacity. J. Hydrol. 535, 54–60. https://doi.org/10.1016/j.jhydrol.2016.01.059.
Wu, W., Kuang, L., Li, Y., He, L., Mou, Z., Wang, F., Zhang, J., Wang, J., Li, Z., Lambers, H., Sardans, J., Peñuelas, J., Geisen, S., Liu, Z., 2021. Faster recovery of soil biodiversity in native species mixture than in eucalyptus monoculture after 60 years afforestation in tropical degraded coastal terraces. Glob. Chang. Biol. 27, 5329–5340. https://doi.org/10.1111/gcb.15774.
Xiao, Y., Yin, S., Yu, B., Fan, C., Wang, W., Xie, Y., 2023. The most extreme rainfall erosivity event ever recorded in China up to 2022: the 7.20 storm in henan province. Hydrol. Earth Syst. Sci. 27, 4563–4577. https://doi.org/10.5194/hess-27-4563-2023.
Xu, Y., Luo, L., Guo, W., Jin, Z., Tian, P., Wang, W., 2024. Revegetation changes main erosion type on the gully–slope on the chinese loess plateau under extreme rainfall: reducing gully erosion and promoting shallow landslides. Water Resour. Res. 60, e2023WR036307. https://doi.org/10.1029/2023WR036307.
Yan, Y., Hu, Z., Wang, L., Jiang, J., Dai, Q., Gan, F., Almaliki, A.H., Hashim, M.A., Hussein, E.E., Ghoneim, S.S.M., 2024. Impact of extreme rainfall events on soil erosion on karst Slopes: a study of hydrodynamic mechanisms. J. Hydrol. 638, 131532. https://doi.org/10.1016/j.jhydrol.2024.131532.
Yang, J., Liu, H., Lei, T., Rahma, A.E., Liu, C., Zhang, J., 2021. Effect of straw-incorporation into farming soil layer on surface runoff under simulated rainfall. Catena 199, 105082. https://doi.org/10.1016/j.catena.2020.105082.
Yang, J.H., Liu, H.Q., Zhang, J.P., Rahma, A.E., Lei, T.W., 2022. Lab simulation of soil erosion on cultivated soil slopes with wheat straw incorporation. Catena 210, 105865. https://doi.org/10.1016/j.catena.2021.105865.
Yue, L., Juying, J., Bingzhe, T., Binting, C., Hang, L., 2020. Response of runoff and soil erosion to erosive rainstorm events and vegetation restoration on abandoned slope farmland in the loess plateau region, China. J. Hydrol. 584, 124694. https://doi.org/10.1016/j.jhydrol.2020.124694.
Zarnetske, J.P., Bouda, M., Abbott, B.W., Saiers, J., Raymond, P.A., 2018. Generality of hydrologic transport limitation of watershed organic carbon flux across ecoregions of the United States. Geophys. Res. Lett. 45, 11702–11711. https://doi.org/10.1029/2018GL080005.
Zhang, X., Wu, K., Fullen, M.A., Wu, B., 2020. Synergistic effects of vegetation layers of maize and potato intercropping on soil erosion on sloping land in Yunnan province, China. J. Mountain Sci. 17, 423–434. https://doi.org/10.1007/s11629-019-5392-0.
Zhao, C., Gao, J., Huang, Y., Wang, G., Zhang, M., 2016. Effects of vegetation stems on hydraulics of overland flow under varying water discharges. Land Degrad. Dev. 27, 748–757. https://doi.org/10.1002/ldr.2423.
Zhao, X., Huang, J., Gao, X., Wu, P., Wang, J., 2014a. Runoff features of pasture and crop slopes at different rainfall intensities, antecedent moisture contents and gradients on the Chinese Loess Plateau: a solution of rainfall simulation experiments. Catena 119, 90–96. https://doi.org/10.1016/j.catena.2014.03.007.
Zhao, X., Huang, J., Wu, P., Gao, X., 2014b. The dynamic effects of pastures and crop on runoff and sediments reduction at loess slopes under simulated rainfall conditions. Catena 119, 1–7. https://doi.org/10.1016/j.catena.2014.03.001.
Zheng, F., 2006. Effect of vegetation changes on soil erosion on the loess plateau. Pedosphere 16, 420–427. https://doi.org/10.1016/S1002-0160(06)60071-4.
Zheng, F., Gu, J., Lu, D., Yang, J., Shuai, X., Li, C., Chen, H., 2024. Mixing with native broadleaf trees modified soil microbial communities of *Cunninghamia lanceolata* monocultures in south China. Front. Microbiol. 15. https://doi.org/10.3389/fmicb.2024.1372128.
Zhou, P., Zhang, X., Tang, K., 2000. Rainfall installation of simulated soil erosion experiment hall of the state key laboratory of soil erosion and dryland farming on loess plateau. Bull. Soil Water Conserv. 27–30, 45. https://doi.org/10.13961/j.cnki.stbctb.2000.04.007.
Zhou, T., Liang, G., Reich, P.B., Delgado-Baquerizo, M., Wang, C., Zhou, Z., 2024. Promoting effect of plant diversity on soil microbial functionality is amplified over time. One Earth. https://doi.org/10.1016/j.oneear.2024.10.004.
Zhu, X., Yuan, X., Lu, E., Yang, B., Wang, H., Du, Y., Singh, A.K., Liu, W., 2023. Soil splash erosion: an overlooked issue for sustainable rubber plantation in the tropical region of China. Int. Soil Water Conserv. Res. 11, 30–42. https://doi.org/10.1016/j.iswcr.2022.05.005.